# THE ELECTROPHYSIOLOGICAL MAPPING OF COMPARTMENTS WITHIN A MAMMALIAN CELL

DANA GIULIAN and ELAINE G. DIACUMAKOS

From The Rockefeller University and Cornell University Medical College, New York 10021

ABSTRACT

The electrical properties of structures within an intact cell were examined by impalement with micropipette electrodes. Mean potential differences (PDs) measured from interphase HeLa cells showed that internal membrane-bounded compartments such as the nucleus, Golgi region, and the mitochondria were more negative than the cytoplasm with respect to an external grounding electrode. The nuclear PDs, unlike Golgi and cytoplasmic PDs, shifted during interphase and reached a peak value shortly before mitosis. The positioning of micropipettes was confirmed by electron microscope examination of marker solutions that were microinjected into specific intracellular regions. The combination of methods described here offers a new approach for the study of physiological events within intact, living cells.

Since the report of Ling and Gerard (16), glass micropipette electrodes have been used extensively to study potential differences (PDs) across the plasma membrane in a variety of cell types. Fluctuations in the electrochemical gradients observed at the plasma membrane, however, are not necessarily related to events that take place within specific intracellular structures. For this reason, electrical measurements obtained directly from a cellular organelle might prove to be more sensitive in monitoring intracellular phenomena.

With the exception of the nucleus in giant salivary gland cells of Drosophila (18), it has not been possible to impale and record from a specific region within a somatic cell. In this study on HeLa cells, we report an experimental approach to permit the recording of PDs from several morphologically distinct intracellular compartments. To confirm the placement of micropipettes, we developed methods using electron microscopy to locate marker solutions microinjected into these compartments.

## MATERIALS AND METHODS

### *Cell Culture and Synchronization*

HeLa cells were cultured in Dulbecco's medium (Gibco Diagnostics, Chagrin Falls, Ohio) with 10% (vol/vol) fetal bovine serum (Flow Laboratories, Inc., Rockville, Md.) heat-treated at 56°C for 30 min (8). Cells were grown on square glass (18 mm, no. 0 thinness, Corning Glass Works, Corning, N. Y.) or plastic (22 mm, Ace Scientific Supply Co., Inc., Linden, N. J.) cover slips. Plastic Petri dishes (no. 3002, Falcon Plastics, Oxnard, Calif.) containing these cover slips were filled with 5 ml of the cell suspension and incubated at 37°C in 5% $CO_2$-95% air atmosphere, at pH 7.4, and 100% humidity.

To isolate a synchronized population of cells, late telophase cell pairs were gently detached by microneedles and then reattached to a centrally cleared area on the cover slip (Fig. 1). After the cell pairs were positioned in a two-dimensional array (Fig. 1), the preparation was returned to an incubator until measurements were taken.

### *Cell Chamber*

Cells adhered to the under surface of a cover slip that

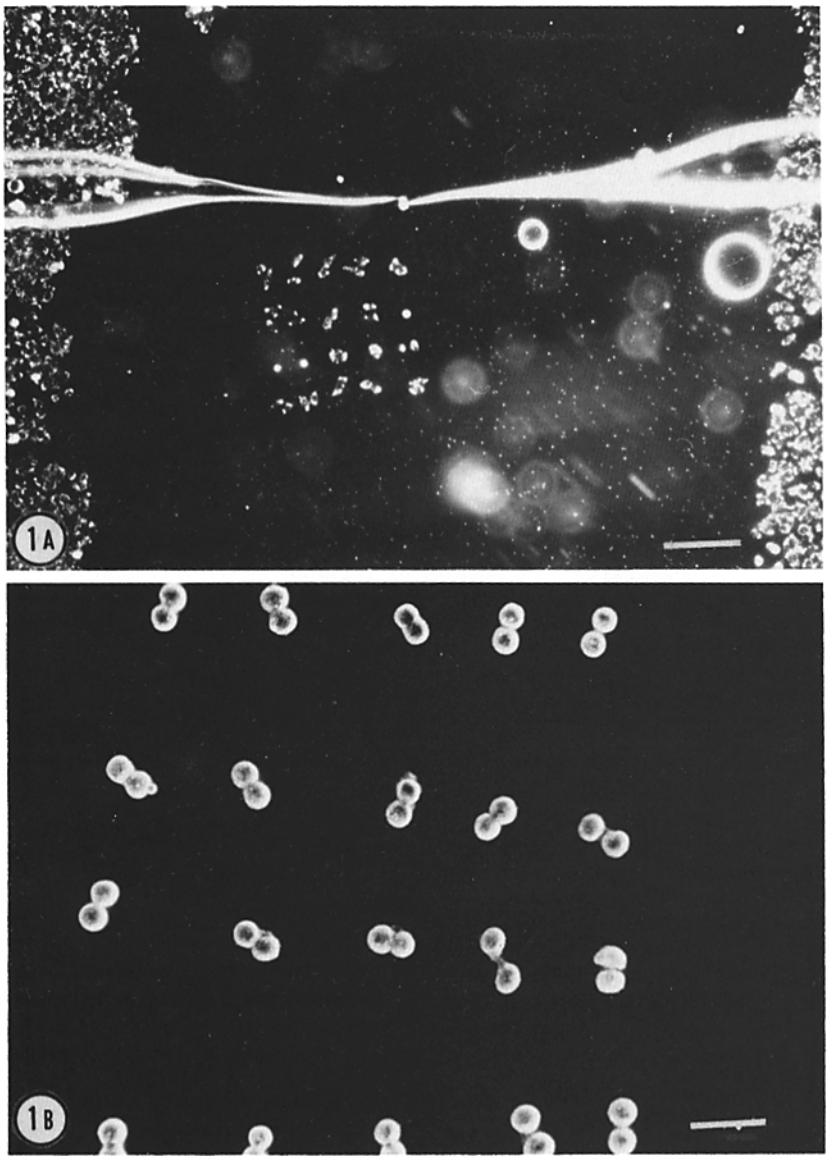


FIGURE 1 (A) Photomicrograph shows the two-dimensional array of telophase cell pairs which are synchronized by selection and transposed to the cleared area in the center of the cover slip. The dense cell population bordering the cleared area and the two microneedles used to position these telophase pairs are evident. × 47. Bar is 200 μm. (B) Higher magnification of a different synchronized cell array. Bar is 50 μm. × 188.

roofed a small glass chamber. This cell chamber, as described previously by Diacumakos (reference 8; Fig. 2), was made of a microscope slide (51 × 76 × 1 mm) on which four 1-mm thick glass supports were cemented in place with Dow Glass Cement (Dow Chemical Co., Midland, Mich.). After securing the cover slip on these supports with Dow silicon vacuum grease, the chamber was filled with culture medium and the four ports were sealed with a layer of sterile silicone oil.

A chlorided silver wire that served as a grounding electrode was immersed in the culture medium through the front port of the chamber (Fig. 2). Chamber fluid temperature was monitored with a glass probe thermistor (0.02 mm diameter, Veeco Instruments, Inc., Plainview,

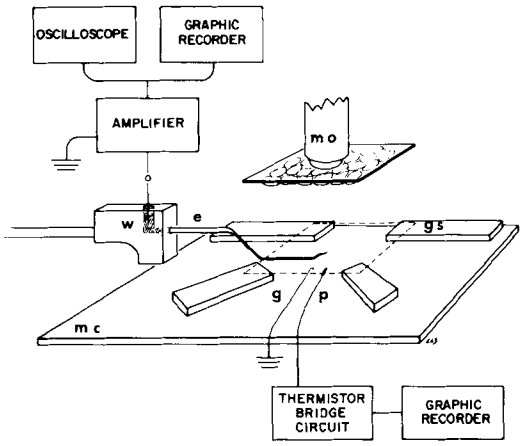


FIGURE 2 This drawing shows the shape and orientation of a micropipette electrode (*e*) as it projects into the cell chamber (*mc*) through a side port. The micropipette is held by a Lucite adapter and is linked to the amplifier input by a well (*w*) containing Ringer's solution. An external grounding electrode (*g*) and thermistor probe (*p*) are shown entering the chamber through the front port. The dotted square superimposed on the four glass supports (*gs*) notes the position of a cover slip that would roof the chamber. In this diagram the cover slip is drawn above the chamber in order to illustrate that cells adhere to its underside while microscope objectives (*mo*) are positioned on its top side. Block diagrams show the arrangement of recording equipment.

N. Y., model Z35A20) linked to Beckman graphic recorder (Beckman Instruments, Fullerton, Calif.) (Fig. 2). A thermistor bridge circuit controlled the response range of the temperature monitoring system. The probe was calibrated over a 25–35°C range in distilled water with a mercury thermometer to the nearest 0.1°C. For experiments reported here, the ambient room temperature was between 27.2 and 30.0°C, and the chamber fluid temperature between 29.5 and 31.1°C.

## *Micropipette Electrodes and Microneedles*

Micropipette electrodes were made from lengths of thin-walled, glass capillary tubes (borosilicate, 0.7–1.0 mm OD) that were soaked in 70% nitric acid and rinsed with tap, distilled, and distilled-deionized water. The capillary tubes were dried and coated with Desicote (Beckman Instruments) (8). Pipettes were filled with either 3 M potassium chloride or 5 M potassium acetate electrode-filling solution.

Two methods were used to make micropipettes. Those drawn on commercial electrode pullers (Industrial Science Associates, Inc., Ridgewood, N. Y., or Scientific Instruments, Inc., Lake Worth, Fla.) were filled with distilled water under reduced pressure for 10 min (15). The micropipettes were then backloaded with Swinnex-filtered electrode solution using a 10-cm, 30-gauge hypodermic needle (Popper & Sons, Inc., New York).

The second method is a modification of the technique described by Diacumakos (8). Capillary tubing was partially drawn out and bent by hand over a microflame. The glass tubing was then positioned in a holder connected to a distilled water-filled syringe and the final bends and tip were produced in a deFonbrune microforge. As the pipette was finished, distilled water was forced through the capillary shaft until it filled the tip. The micropipette was then backloaded with electrode solution and allowed to equilibrate for several hours before testing.

All microelectrodes when immersed in Dulbecco's medium showed relatively low noise with tip resistances between 22 and 55 MΩ and tip potentials less than 3 mV (1). These electrical characteristics are similar to the properties of intracellular glass pipettes used by many other investigators (15). The end of the micropipette tips were visible (Fig. 11) allowing visual control during electrode positioning.

Microneedles were made from 1-mm borosilicate glass rods and finished on the microforge (8).

## *Electrical Recording and Phase Microscopy*

The recording system included a negative capacitance, high input impedance preamplifier[1] with a gain of 10. Potential measurements were observed on a Tektronix type 502A dual-beam oscilloscope and plotted on a Brinkmann W + W recorder (Brinkmann Instruments, Inc., Westbury, N. Y.). The grounded micromanipulator, microscope, and baseplate were housed in a grounded sheet-metal hood, open on one side. Small, adjustable metal shields with hinged arms were also used to isolate electrically the front of the microscope stage.

Tip resistances were measured by balancing an internal bridge circuit and tip potentials were nulled by a bucking circuit.

The micropipette electrodes were held by Lucite adapters (Fig. 2) mounted in Leitz micropositioners. A chlorided silver wire dipping into an adapter compartment (filled with Ringer's solution) linked the microelectrode to the preamplifier input. A second chlorided silver wire, as noted before, served as a grounded reference electrode.

To reduce vibrations, the micromanipulator was shock-mounted on two heavy iron plates separated by thick-walled rubber tubing (8). Air currents were reduced by the adjustable metal shields placed in front of the microscope. The only mechanical link between the preparation and the preamplifier was the silver wire dipping into the chamber of the adapter.

Cells were observed with oil immersion phase-contrast optics at 1,875 magnification (Fig. 2), using a Laborlux

[1] Designed and built by Michelangelo Rossetto of The Rockefeller University Electronics Laboratory.

II microscope (E. Leitz, Inc.). Impalement was achieved by raising the microelectrode tip into the cells.

A built-in light source (Osram, 6 V, 15 W) was controlled by a regulated power supply to reduce 60 Hz noise (model 809A; Harris Laboratories Inc., Lincoln, Neb.). Photographs were taken with a Leitz photographic attachment on Panatomic-X, 35 mm film.

### *Microinjection and Electron Microscopy*

Both iontophoresis and pressure injection techniques were used to place electron-dense markers within intracellular regions. In either case, the micropipettes were finished on a deFonbrune microforge and backloaded with a solution of marker material under controlled pressure as the tips were drawn out.

Procion brown (4% wt/vol) and cobalt chloride (50 mM) solutions were iontophoretically injected by single or multiple current pulses (13). Pulses were generated by the Tektronix 160 series (type 162 Waveform Generator, type 161 Pulse Generator) and a stimulator[2] (current range 1–10 × $10^{-9}$ A, pulse duration 0.5–2 s). Single pulse iontophoresis was carried out with a current injection system (about $10^{-7}$–$10^{-6}$ A).

Solutions of ferritin, myoglobin, or Procion brown, and a suspension of colloidal thorium dioxide (Thorotrast) were microinjected under pressure. The thorotrast particles range in size from 50 to 200 Å (10). The injection system, as described by Diacumakos (8), consisted of a micrometer-driven, gas-tight Hamilton syringe (LT1002) connected to a micropipette holder by stainless steel capillary tubing.

Cells injected for electron microscope examination were grown on plastic cover slips. Groups of two to six injected cells were identified by clearing away unwanted cells and by scratching lines into the plastic cover slip around the cell cluster (Fig. 3). The time interval between injection and fixation was noted for each cell.

Cells on cover slips were fixed at room temperature for 20 min in 2% glutaraldehyde (Fisher Scientific Co., Pittsburgh, Pa.) in 0.1 M cacodylate buffer (pH 7.4). After rinsing in Veronal acetate buffer (pH 6.8), cells were treated with 1% osmium tetroxide (in Veronal acetate buffer) for 60 min, followed by a second acetate buffer rinse. Cells were poststained for 60 min in 0.25% uranyl acetate in acetate buffer, and dehydrated in a graded ethanol series followed by three 10-min washes in absolute ethanol. Propylene oxide dehydration was omitted because of the plastic cover slips.

The cover slip was next placed on an Epon-filled gelatin capsule that had been heated to drive air bubbles out of the Epon. After 4 h in an oven at 70°C, the plastic cover slip was pulled away from the hardening Epon block and the block was returned to the oven for at least 12 h more. Block trimming, aided by the scratch marks now molded in the Epon, was carried out using a Wild dissecting microscope at 100 magnification.

Thin sections were cut with a diamond knife on a Porter-Blum microtome. Since the cells reached the surface of the Epon, it was necessary to examine the first sections that were cut from the block. In most cases sections were not stained to facilitate recognition of the injected markers. Cells were viewed with a Siemens-Elmiskop 1 electron microscope operated at 80 kV.

## RESULTS

Fig. 4 presents the principal features of interphase HeLa cells as seen with phase-contrast optics at 1,875 magnification. The nucleus may show several nucleoli and is elliptical in different focal planes. A region that lies adjacent to the nucleus as a cluster of vesicles or as a lighter but distinct portion of the cytoplasm contains the Golgi apparatus[3] as demonstrated by phase-contrast and UV microscopy (7, 20, 22), cytochemical straining (7, 26), and electron microscopy (2, 3, 27). Mitochondria are seen as elongated dark bodies, variable in length and 2 μm or less in diameter, and are readily distinguished from other granular or inclusion bodies (19, 20).

To record from membrane-bounded intracellular regions, it was first necessary to develop electrodes suitable for impaling fragile structures with diameters of 1–2 μm. Microelectrodes drawn on commercial pullers and then bent in the microforge could be used to impale either the nucleus or the cytoplasm. An initial negative transient was observed upon penetration of the plasma membrane, and a second sharp transient upon tip entry into the nucleus. Such micropipette electrodes, though appearing small enough at the tip, were often unsatisfactory due to the angle, shape, or size of the pipette shaft, which hindered placement or caused excessive cell damage. Accordingly, the majority of microelectrodes used in this study were hand-drawn and finished on a deFonbrune microforge for they showed uniform tip and shaft configurations more suitable for precise impalements.

To reduce the major artifacts that accompany any type of intracellular recording technique, such

[2] Designed and built by The Rockefeller University Electronics Laboratory.

[3] Light microscopists also refer to this region as the nuclear hof or cytocenter. A discussion of the historical controversy surrounding the description of Golgi's "inner reticular apparatus" as viewed by light and electron microscopy may be found in reference 27.

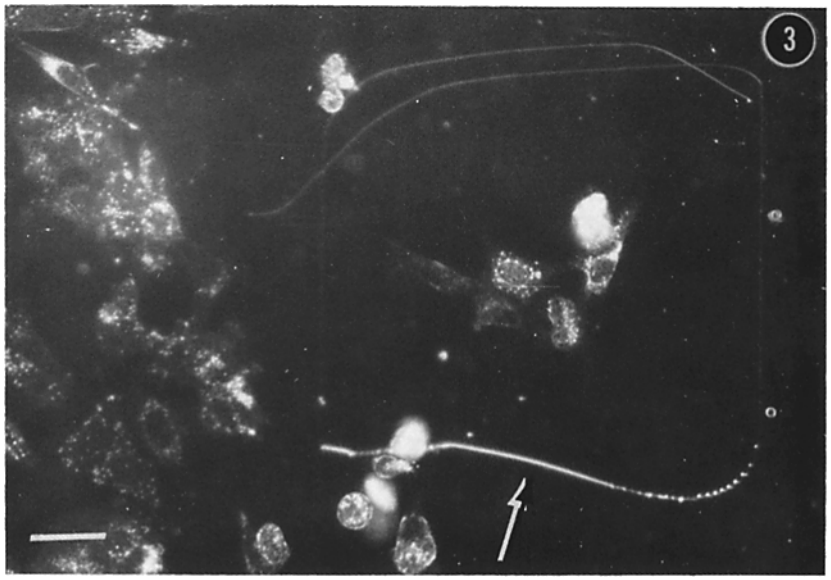


FIGURE 3 Each cell within this group of six interphase cells has been microinjected for electron microscope examination. The scribed line (arrow) that was etched into the plastic cover slip with the shaft of a broken microneedle facilitates the relocation of the cells. Bar is 50 μm. × 188.

as unstable tip potentials or cell damage,[4] we selected the following criteria for a successful measurement: (*a*) a rapid transient recorded upon entry of the microelectrode tip into a specified cell region; (*b*) a stable PD recorded for at least 10 s; (*c*) a rapid transient upon withdrawal of the electrode tip from that cell compartment; (*d*) restoration of tip potential to base-line level upon removal of the microelectrode from the cell; and (*e*) maintenance of stable tip resistance during the impalement. The PD between the grounded base-line level and the 10-s plateau were determined from the graphic records.

Cells were continuously observed during the impalement to ensure maintenance of the position of the microelectrode tip. Data were discarded if the cells did not remain intact and viable or if they showed extensive blebbing during or immediately after impalement. On occasion, the microelectrode tip became coated with cellular material or with an impaled cell that was inadvertently pulled free from the cover slip. This debris was removed electrically by brief current pulses, or mechanically by microneedles. Microelectrodes cleaned in this way were rechecked and replaced if any shift in base-line tip potential or tip resistance was seen.

### *Electrical Measurements from Asynchronous Interphase Cells*

Interphase cells were selected from among the cell population on the cover slip solely on the basis of their accessibility for impalement. When organelles were properly aligned relative to the advancing microelectrode tip, it was possible to enter several different compartments of one cell after a

[4] As with any micropipette technique, a shunt may occur at the site of membrane puncture. We describe here the PD as a stable potential level obtained from a morphologically intact structure while recognizing the inherent uncertainty of this value that arises from membrane penetration (11).

FIGURE 4 Photomicrographs of three different interphase HeLa cells illustrate the major intracellular structures observed with oil immersion phase-contrast optics. The Golgi region (A and B) appears as an aggregate of clear vesicles in a perinuclear position. Elongated mitochondria are clearly visible (B and C) and easily distinguished from various granules and lipid droplets. Nucleus (*N*); nucleolus (*n*); Golgi region (*G*); mitochondria (*M*); Cytoplasm (*C*) and lipid droplets (*L*). × 1875. Bar is 5 μm.

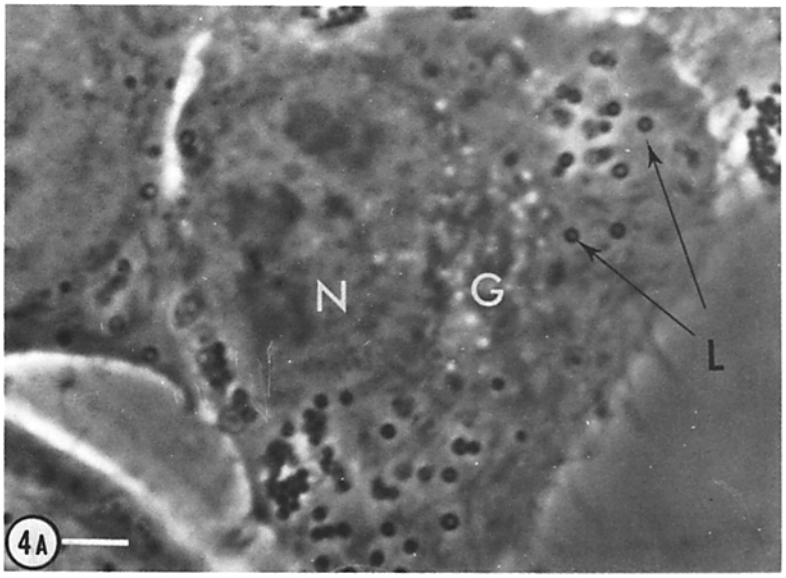


4A

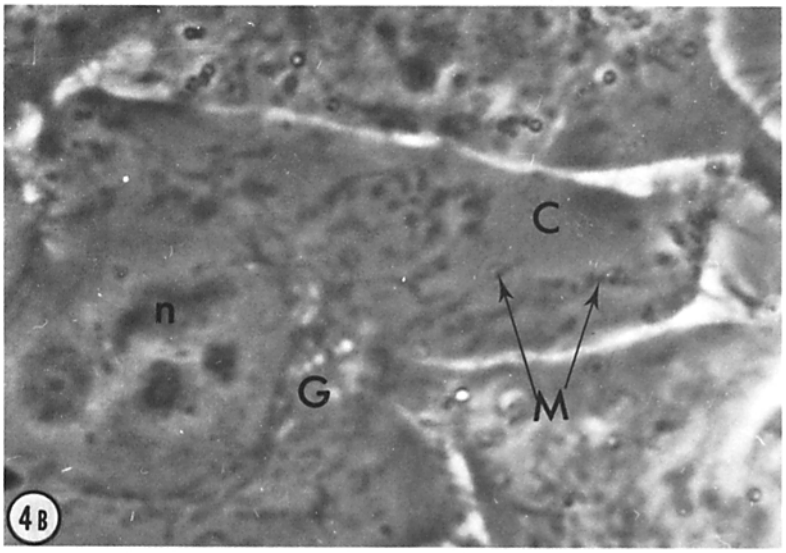


4B

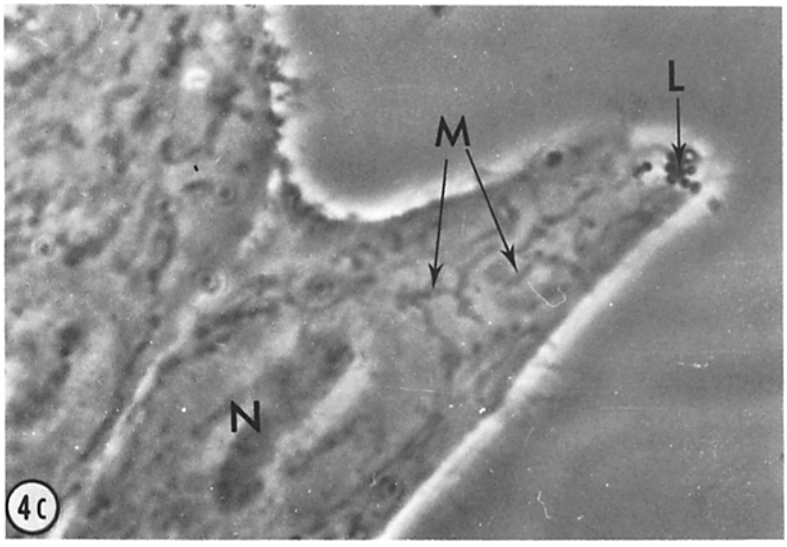


4C

single penetration of its plasma membrane. Generally, this was not the case and a different region of the same cell was reached only by a second impalement.

The cytoplasmic PD was measured by penetrating the plasma membrane and advancing the microelectrode tip deeper into the cell without touching visible organelles. A typical record from a cytoplasmic impalement is shown in Fig. 5, for a single penetration; the trace in Fig. 6 follows a nuclear recording.

Such multiple punctures were possible, particularly if care was taken to keep the plasma membrane intact by restricting microelectrode motion to simple in-and-out movements. Cytoplasmic PDs decayed rapidly if the outer membrane was torn by a microneedle as the measurement was taken. A total of 72 successful impalements gave a mean value of $-10.0 \pm 0.5$ mV (Table I). These data show close agreement with values from similar cell culture lines obtained by conventional recording techniques (3–5, 25).

An example of a PD recorded from the Golgi region is shown as part of the trace in Fig. 6. Fig. 7 demonstrates the positioning of the microelectrode tip for such measurements. Golgi penetrations often produced multiple sharp transients as the electrode tip was advanced, suggesting that membrane layers within this region may be traversed. The mean PD from 42 Golgi measurements was $-23 \pm 1.5$ mV (Table I).

Measurements from mitochondria, the smallest visible compartments impaled, were made with gradually tapered, very fine-tipped micropipette

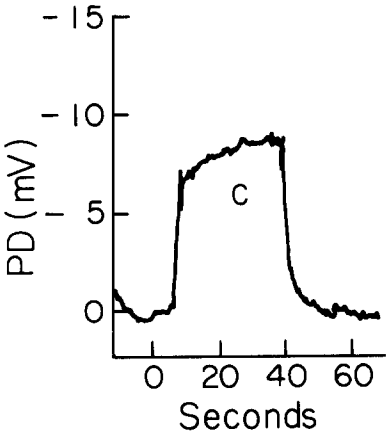


FIGURE 5 A record of the cytoplasmic PD with respect to an external grounding electrode upon a single penetration of the plasma membrane.

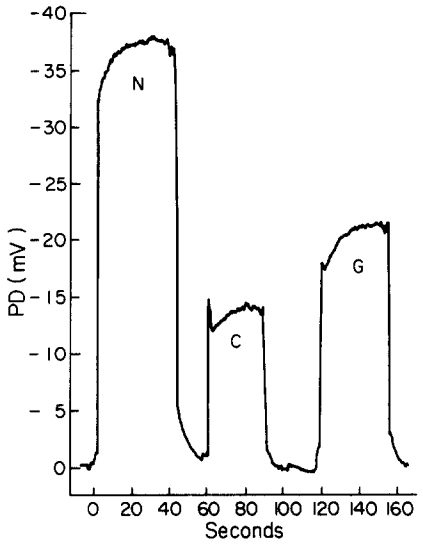


FIGURE 6 A trace of the PDs is shown during a sequence of multiple impalements into the nuclear (N), cytoplasmic (C), and Golgi regions (G) of an individual cell. Each intracellular compartment was reached by a new penetration of the plasma membrane.

electrodes. Sharp negative transients appeared as the electrode tip was moved from the cytoplasm into the mitochondrion. If the electrode tip was advanced through the mitochondrial wall opposite the site of entry or if the tip was retracted back into the cytoplasm, the PD returned to the cytoplasmic level. Fig. 8 is a mitochondrial PD recorded during the second impalement of the plasma membrane. In Fig. 9, a mitochondrial impalement was followed immediately by a nuclear puncture. A mean PD value of $-21.0 \pm 1.0$ mV was obtained from a total of 34 mitochondrial measurements.[5] The photomicrograph (Fig. 10) illustrates the selective penetration of a mitochondrion.

Comparisons (Student's $t$ test) of the mean PD values of cytoplasm, Golgi apparatus, and mitochondria are listed in Table II. The mean PDs from the Golgi region and mitochondria are significantly more negative than that of cytoplasm ($P < 0.001$) but are not significantly different from each other.

Electrical records for nuclear impalements are shown in Figs. 6, 8, and 9. The position of the

[5] Tupper and Tedeschi (28) have reported electrical data from isolated Drosophila mitochondria. They found PDs of about +10 mV with impalements lasting 0.1 s.

TABLE I

*Mean PDs ± SEM with Respect to an External Grounding Electrode Obtained by Direct Micropipette Electrode Impalement of Intracellular Regions from Randomly Selected Interphase HeLa Cells*

| Region | Number of impalements | Mean PDs ± SEM |
|---|---|---|
| | | *mV* |
| Cytoplasm | 72 | −10.0 ± 0.5 |
| Golgi region | 42 | −23.0 ± 1.5 |
| Mitochondrion | 34 | −21.0 ± 1.0 |
| Nucleus | 69 | −43.5 ± 1.5 |

electrode tip for such measurements is illustrated in Fig. 11. Advancing the electrode tip through the nucleoplasm produced no additional transients such as those seen during Golgi impalement. The nuclear PD decayed to cytoplasmic level when a microneedle was used to puncture and tear the nuclear envelope by lateral displacement.[6] The mean value for 69 nuclear PD measurements was −43.5 ± 1.5 mV.[7]

Impalement of intracellular compartments required, of course, the penetration of the plasma membrane. However, as seen in the traces presented here, rapid punctures of the organelles did not show a distinct cytoplasmic PD due to the slow response time of the graphic recorder. In some cases (Fig. 9), a shoulder seen on the initial transient represents an obscured record of the outer membrane penetration.

Fig. 12 is a frequency histogram of intracellular measurements collected from asynchronous interphase cells. Data from cytoplasmic, Golgi, and mitochondrial impalements distributed into single peaks. Nuclear data, however, showed peaks at −30 to −40 mV and at −50 to −60 mV, and might reflect two classes of interphase HeLa nuclei.

## *Electrical Measurements during the Growth of Synchronized Cells*

A possible relationship between nuclear PDs and the cell cycle was studied by measuring cells at different times during interphase. Grouping of selected telophase pairs within a cleared area of the cover slip (Fig. 1) provided a synchronized starting point and a means of unequivocally identifying each cell of each pair. No differences in potential levels were observed between telophase pairs studied at random and those telophase pairs that had been transposed. In this set of experiments, mitochondrial measurements were not attempted because these organelles were not readily accessible during our first time-point. Moreover, the experimental design differed from earlier ones in that the cells were preselected before they had spread on the cover slip and therefore did not show optimal orientations for impalement.

Late telophase was selected as $t = 0$ h. Subsequent measurements were taken at 5-h intervals, with each array of cells used only for one time-point. Single or multiple impalements of a cell were carried out, depending on the cell's geometry with respect to the microelectrode. For each data point presented, we obtained a mean value of not less than 18 impalements taken from at least three different cover slip preparations. As shown in Fig. 13, the cytoplasmic and Golgi PDs were relatively stable throughout interphase. In contrast, the nuclear levels varied with a plateau of about −34 mV from $t = 5$ to $t = 15$ h and peak of about −51 mV at $t = 20$ h.

The viability of these cells was monitored by returning the cell chamber with the cover slip preparation to an incubator immediately after measurements were made. We found that, of 24 cells which had received multiple punctures at $t =$ 10 h, 22 (92%) remained viable for the next 24 h and that, of these, 6 (25%) showed cell replication within the normal cell cycle time.

Our results suggest that it is feasible to examine the electrical properties of various organelles from one cell for an extended period of time.

## *Placement of Markers within a Cell*

To demonstrate the ability to impale specific regions within a cell, we sought to inject intracellular compartments with markers that could be located by electron microscopy. Microinjection at this level is a more complicated technique than simple impalement. In addition to the precise control required for injection, the selection of appropriate electron-dense markers and the relocation of injected organelles for electron microscope examination presented additional technical problems.

[6] Loewenstein and Kanno (17, 18) have examined the electrical properties of nuclei found within large Drosophila salivary gland cells. These cells contain nuclei between 30 and 40 μm or about twice the diameter of the entire HeLa cell used in this study.

[7] The standard error of the mean was computed despite the apparent non-Gaussian distribution of the nuclear measurements.

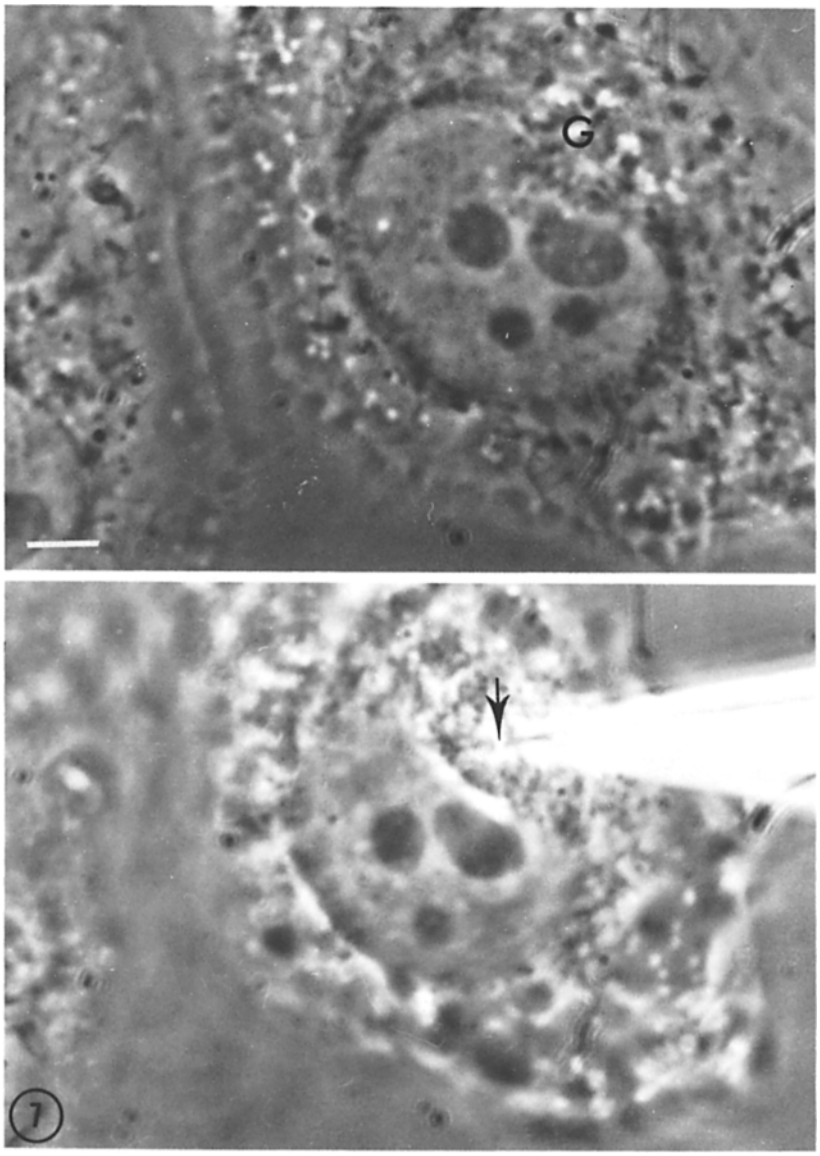


FIGURE 7 These photomicrographs show an interphase cell before and during the positioning of a microelectrode (arrow) within the Golgi region (*G*). The electrode is in the cell below the level of the cover slip. × 1875. Bar is 5 μm.

Injections of 4% Procion brown or 50 mM cobalt chloride solutions were carried out iontophoretically (13). Multiple bursts of small current pulses (~$5 \times 10^{-9}$ A every 1–2 s; 1 Hz) made dye visible during cytoplasmic or nuclear injections, although only after periods as long as 30 min. The rate of filling could be increased by breaking the pipette tip to provide a larger orifice, but this technique impaired the control of tip placement. Since a prolonged mitochondrial or Golgi impalement might result in destruction of the organelle, a few bursts of large single pulses of current (~$10^{-6}$ A) were applied to reduce the injection time. This method, however, produced extensive cytological damage.

Single step-controlled pressure injections were found to be more suitable for staining intracellular compartments. Trials with a variety of electron-

dense markers including Procion brown, ferritin, and myoglobin showed that the largest marker employed, a suspension of thorium dioxide particles (50–200 Å, Thorotrast), was the material most readily identified by electron microscopy.

Electron micrographs of Thorotrast pressure-injected into cytoplasm and mitochondria illustrate these results. Cytoplasmic injections showed a scattered, dispersed pattern of thorium dioxide particles (Fig. 14). Cells responded to larger injections with a characteristic blebbing at the periphery as observed with phase optics. These blebs, in electron micrographs, appeared as islands with dense collections of particles (Fig. 14). Smaller injections of Thorotrast did not produce blebbing. Cells fixed within 15 min after injection showed particles freely dispersed throughout the cytoplasm and not collected within membrane-bounded regions (2).

Microinjections into mitochondria necessarily involved transfer of much smaller volumes of fluid. Therefore, fewer thorium dioxide particles were visible with this type of staining than with a cytoplasmic one. Successfully injected mitochondria often appeared slightly larger and darker with phase-contrast optics, while the surrounding cytoplasm was unaffected. Electron micrographs showed that the thorium dioxide generally appeared as a small cluster of particles within the mitochondrial matrix or as a collection of particles

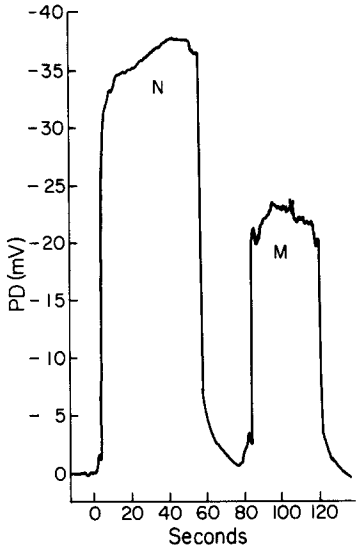


FIGURE 8 A trace of PDs recorded from the nucleus (N) and mitochondrion (M) by two different penetrations of the plasma membrane of an individual cell.

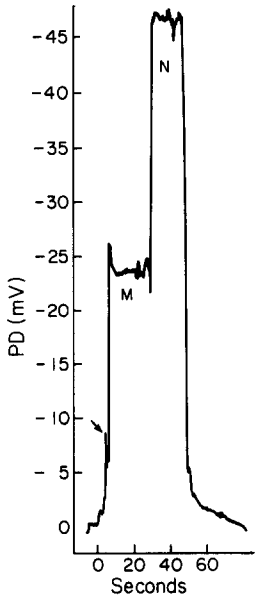


FIGURE 9 A trace of PDs recorded from a mitochondrion (M) and the nucleus (N) by one penetration of the outer membrane of an individual cell. In this example, the microelectrode tip is advanced directly from the mitochondrion into the nucleus. The arrow indicates an obscured record of the cytoplasmic PD as the microelectrode moves from the cell's surface into the mitochondrion.

within a ring-shaped membrane structure inside a mitochondrion (Figs. 15 and 16).[8] If the volume of Thorotrast injected into mitochondria was too large or its transfer too sudden, the organelles appeared to burst, releasing their contents into the cytoplasm. Electron micrographs support these phase-contrast observations, showing mitochondrial damage and thorium dioxide particles dispersed throughout the cytoplasm.

Placement of micropipettes within the Golgi apparatus or the nucleus is clearly shown in the phase-contrast micrographs of Figs. 7 and 11. Injections into nuclear and Golgi regions were easily distinguished from those into cytoplasm by elec-

[8] Electron-dense particles are found within mitochondria from a variety of cell types (23). In this study, uninjected control HeLa cells without poststaining of the sections showed only occasional, round granules within the mitochondrial matrix. Thorium dioxide particles injected into mitochondria are readily distinguished from such granules by their greater electron density, larger size, and irregular edges. Furthermore, thorium dioxide particles distribute as clusters or within ring structures.

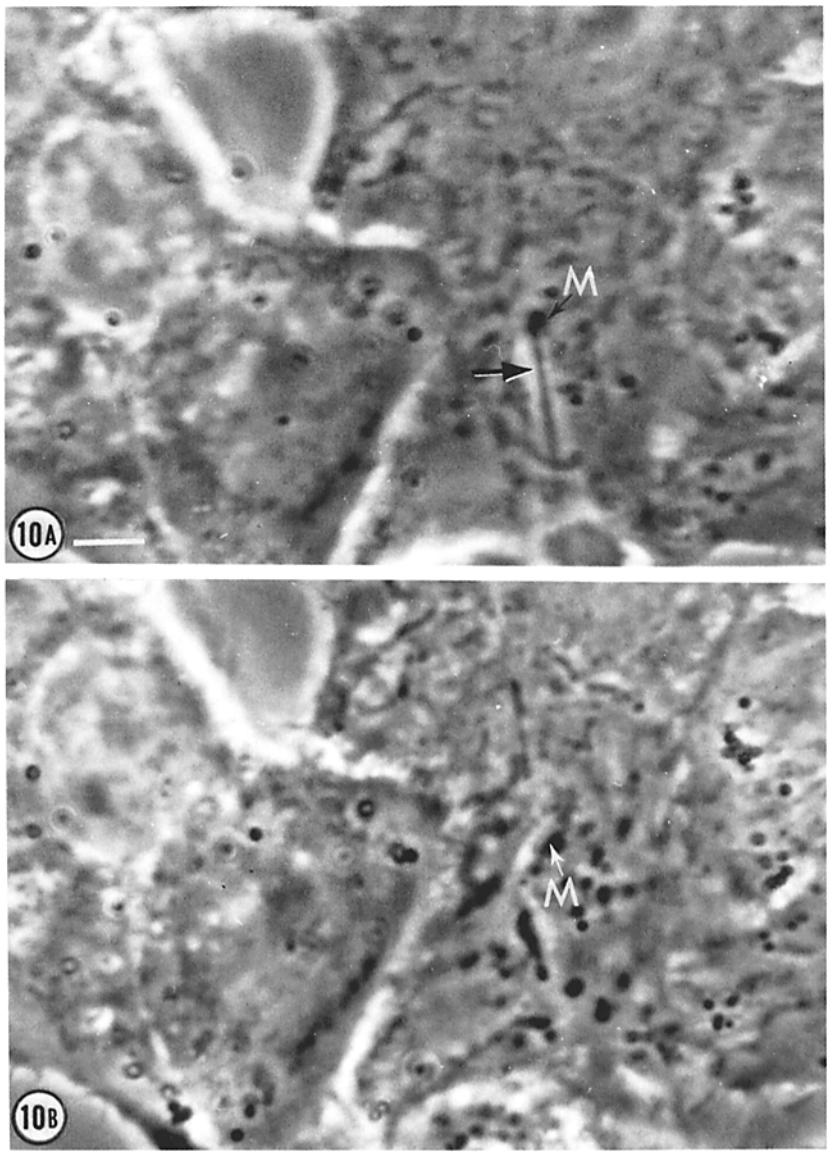


FIGURE 10 Photomicrograph of an interphase HeLa cell during (A) and immediately after (B) impalement of a mitochondrion (*M*). The micropipette shaft (arrow) is visible as it enters the mitochondrion from the bottom of the photograph. × 1875. Bar is 5 μm.

TABLE II

*Comparisons of Mean PDs from Intracellular Regions within Asynchronous Interphase HeLa Cells Through an Analysis of Data by Student's t Test*

| Compartments | *t* | *df* | *P* < |
|---|---|---|---|
| Cytoplasm vs. Golgi region | 8.22 | 112 | 0.001 |
| Cytoplasm vs. mitochondrion | 9.84 | 104 | 0.001 |
| Golgi vs. mitochondrion | 1.13 | 74 | NS |

tron microscopy and demonstrate compartmental impalement. These results will be presented elsewhere.[9]

## DISCUSSION

For the most part, electrophysiological study of transmembrane phenomena has relied upon intra-

[9] Giulian, D. and E. G. Diacumakos. Manuscript in preparation.

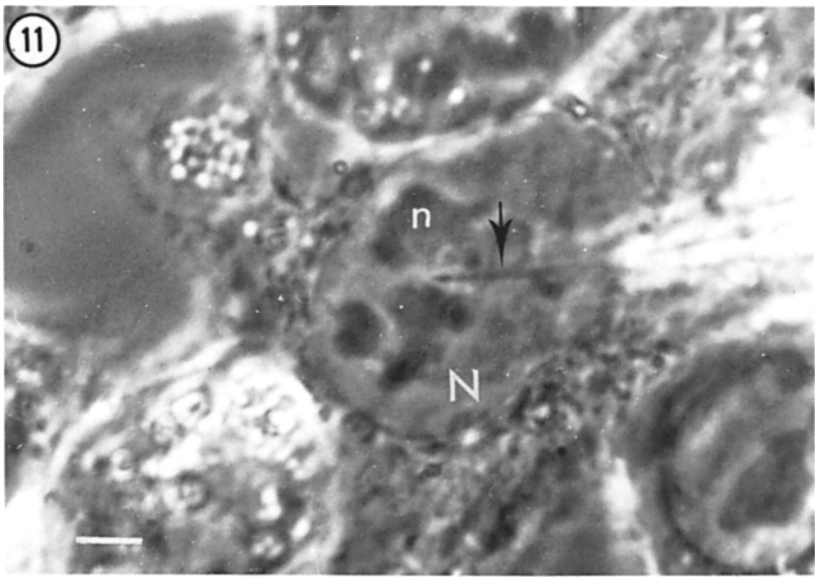


FIGURE 11 The nuclear impalement of a HeLa cell in the center of the photomicrograph is shown. The micropipette shaft (arrow) is seen entering the nucleus from the right side. Nucleus (*N*); nucleolus (*n*). × 1875. Bar is 5 μm.

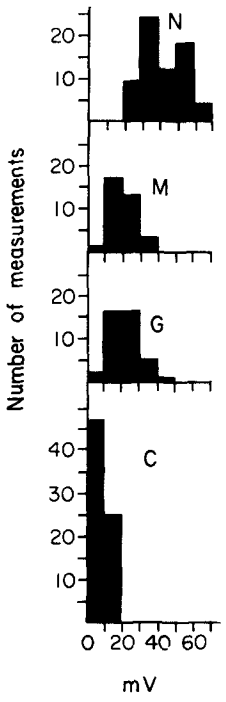


FIGURE 12 The histogram shows the frequency distribution of PDs measured from intracellular regions within asynchronous interphase HeLa cells.

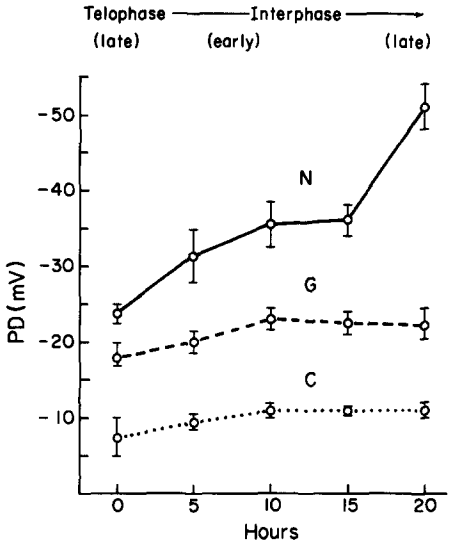


FIGURE 13 Comparisons of mean PDs (±SEM) measured from intracellular regions within synchronized cells at different time-points during the cell cycle. Data for each time-point include at least 18 impalements from three or more cover slip preparations.

cellular PDs measured by microelectrodes placed randomly within a cell. Necessarily, the models arising from such data treat a cell simply as a

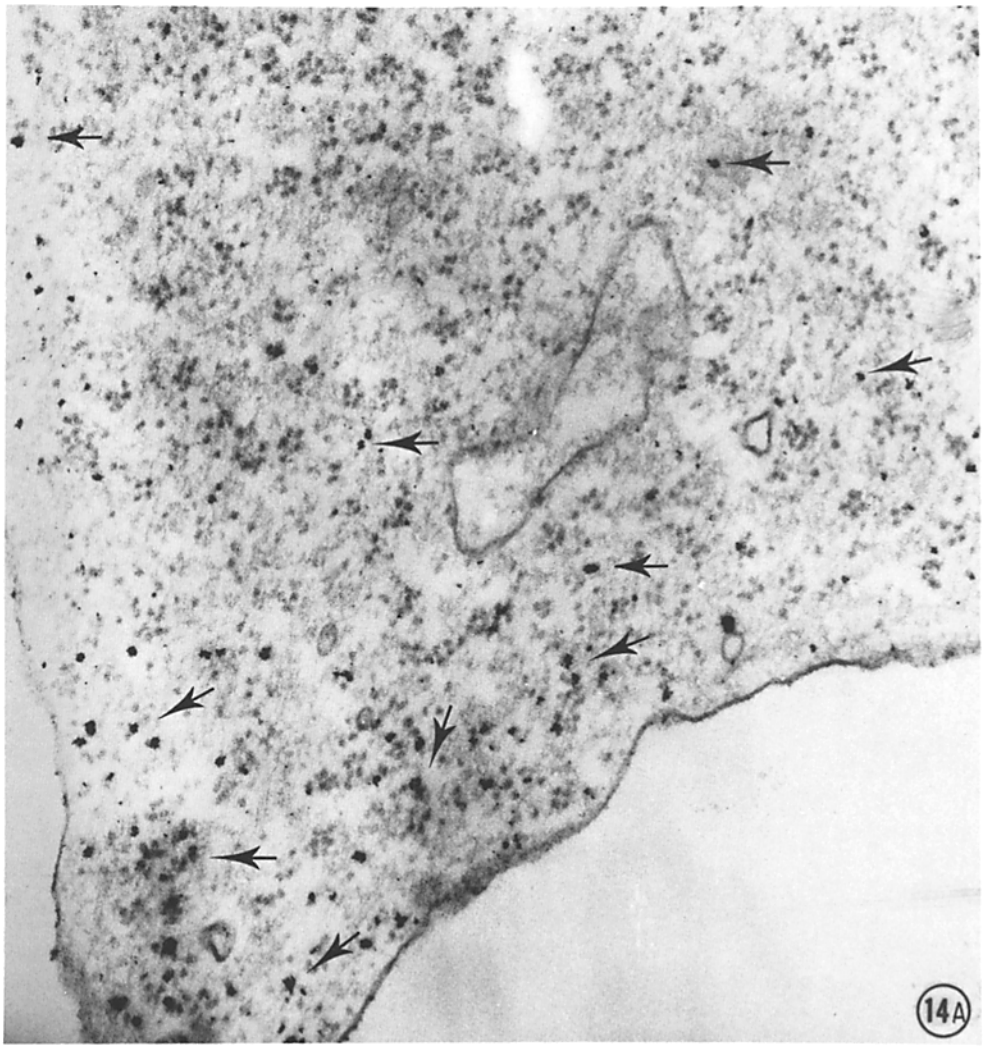


FIGURE 14 (A) An electron micrograph showing dispersal of thorium dioxide (arrows) particles after pressure microinjection of Thorotrast into the cytoplasm. Particles are freely distributed near the outer membrane and are not collected in vesicles × 37,500.

homogeneous body surrounded by a plasma membrane. There develops an obvious gap between the knowledge of organelle function and the involvement of transport mechanisms and electrochemical gradients in these functions. One limitation has been the inability to impale internal membrane structures selectively. We report here for the first time the systematic measurement of potential levels from different intracellular compartments—the cytoplasm, the Golgi apparatus, the mitochondria, and the nucleus—of an intact cell. The reliable placement of microelectrodes into different regions of the cells has been demonstrated by their characteristic potential levels and by phase-contrast micrographs of microelectrode positioning. We confirm these results by electron microscopy of precisely directed microinjections of suitable markers.

We found that an interphase HeLa cell contains regions that are heterogeneous in their electrical properties. It is reasonable that these data are representative of many cell types since the HeLa line, with its common size, ultrastructure, and biochemistry, has served as a model for mamma-

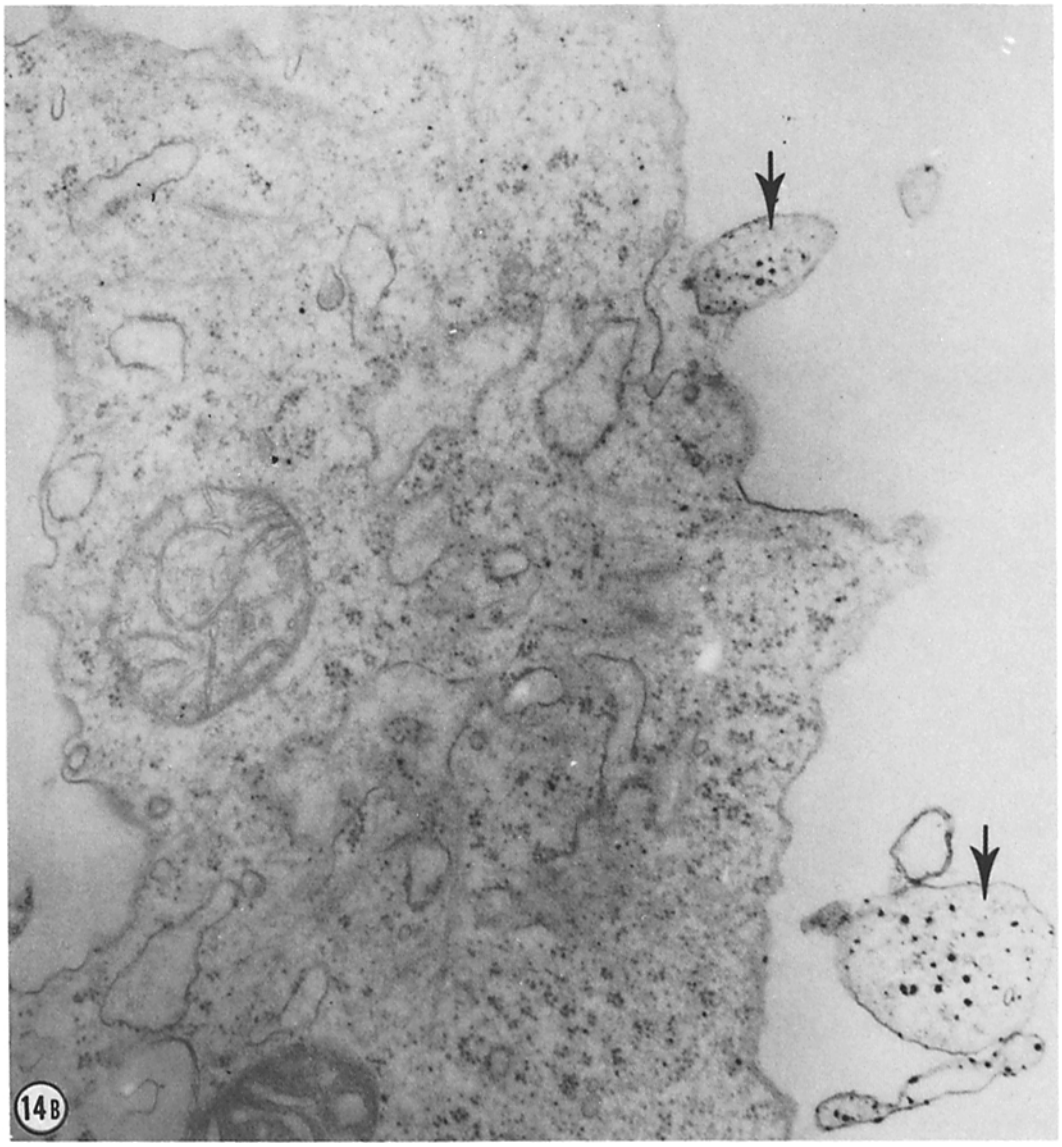


FIGURE 14 (B) A cytoplasmic microinjection of large volumes of Thorotrast. With phase optics, cells showed characteristic blebbing at the periphery. These blebs appear in thin sections as islands with dense collections of thorium dioxide particles (arrows). The sections are unstained. × 24,000.

lian somatic cells (9). Internal membrane-bounded structures showed characteristically more negative PDs than the cytoplasm with respect to an external grounding electrode. During interphase, the nucleus was more negative than the Golgi region or the mitochondria. It was apparent that the PDs were dependent upon membrane containment as suggested by the rapid sharp transients seen during membrane penetration and by the fact that tearing of membranes with microneedles caused an immediate loss of PDs (17, 18). Moreover, we observed multiple sharp transients as microelectrodes advanced through the Golgi region which contains layers of membranous cisternae. In contrast, only single transients were found upon penetration of the nuclear envelope despite microelectrode movement throughout the nucleoplasm.

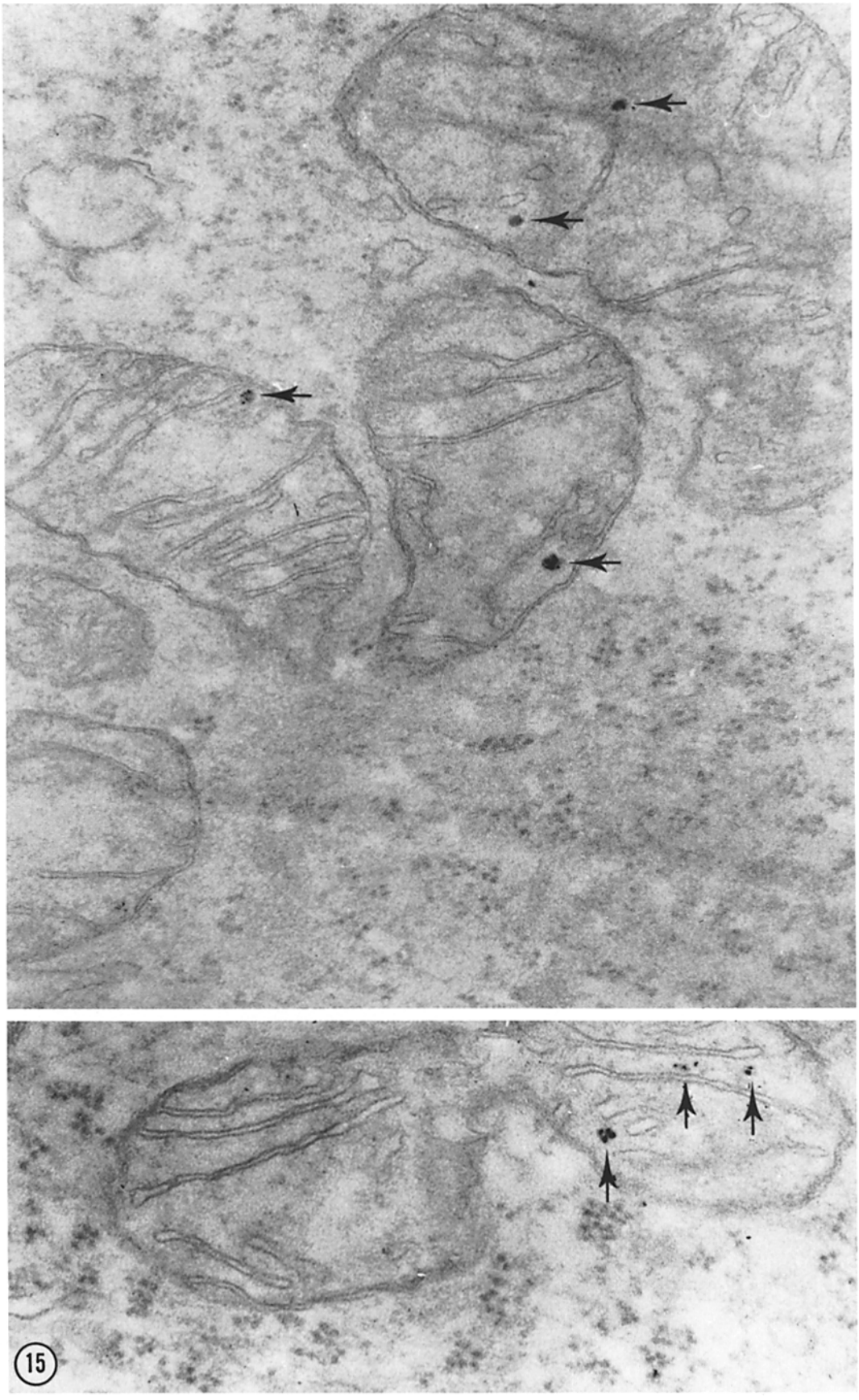

15

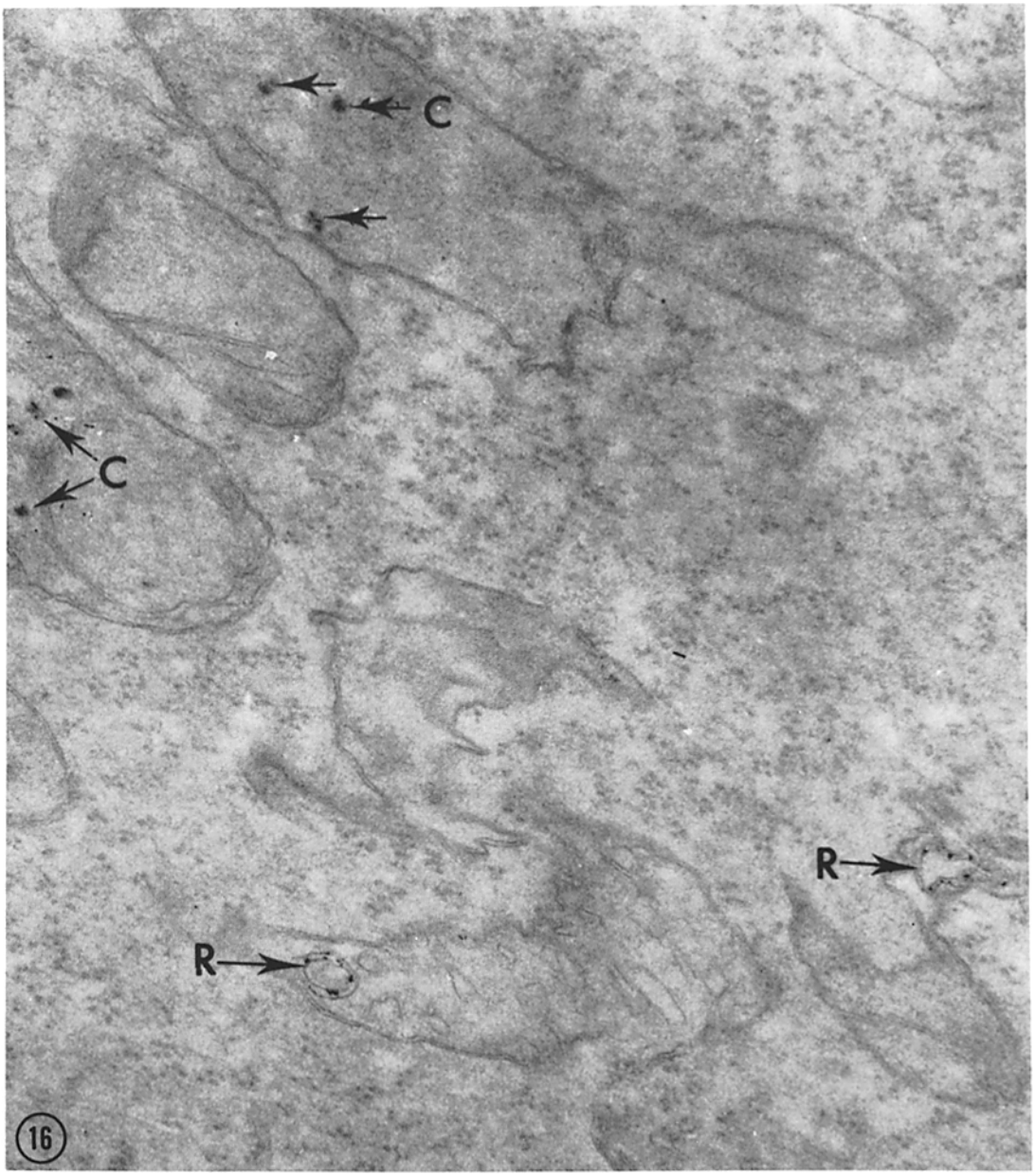


FIGURE 16 Localized mitochondrial injection showing thorium dioxide particles in clusters (*C*) in the mitochondrial matrix or in ring-like (*R*) membrane structures. Section is unstained. × 35,000.

FIGURE 15 Two micrographs showing clusters of thorium dioxide particles injected into a mitochondrion (arrows). In such localized injections, particles are not found dispersed in the cytoplasm. Sections are unstained. × 33,000.

Speculation on the electrical properties of mitochondria within a cell has received some attention because of the extensive study on selective membrane permeabilities of isolated mitochondria. These theoretical calculations of PDs vary over a wide range (−270 to +37 mV; references 6, 12, 21) and in general do not agree with the polarity or order of magnitude of the direct measurements reported here. We suggest that data based upon observations made on cellular components that have been removed from their normal cytoplasmic environment might not reflect a true physiological state.

A histogram of measurements obtained from randomly selected interphase cells shows that the nuclear values, unlike other intracellular values, appeared to distribute into two classes. Examination of interphase cells from known points in the cell cycle indicated that the nuclear PD was cell-age dependent with a peak interphase level just before mitosis. Our results, which demonstrate the nuclear envelope as an intracellular barrier with changing transmembrane potentials, support the hypothesis that specific electrochemical gradients are established within a cell during particular biosynthetic events (14, 24). Moreover, transport phenomena measured across the plasma membrane are not of themselves sufficient to account for the distinctive intracellular features reported here.

The ability to measure stable PDs from specific regions within a cell suggests that it is feasible to carry out other conventional electrophysiological measurements at this level. For example, it will be interesting to monitor ionic distributions within organelles during the propagation of an action potential or perhaps after hormonal stimulation.

The electron micrographs of microinjected cells are presented here to confirm selectivity of micropipette positioning. A good correlation exists between various micromanipulations carried out with phase-contrast microscopy and the ultrastructural consequences demonstrated by electron microscopy. It becomes possible, therefore, to test by microinjection the effects of many biologically active substances on selected intracellular sites. In a similar way, insertion of probes, labels, or drugs would allow analysis of transport and biosynthetic events within single organelles.

At present, most investigations of intracellular events employ either histological examination of fixed preparations or the biochemical study of isolated cell parts. There is, of course, a significant loss of information since such experimental methods cannot monitor ongoing processes within a cell. For this reason, the techniques described here offer a unique opportunity to elucidate physiological relationships between selected organelles.

We acknowledge the assistance of Mr. William A. Duncan, III, Miss Edith Espiritu, and Miss Susan O'Rourke in preparing materials and cell cultures. We are grateful for the enthusiastic support of the late Dr. Edward L. Tatum. We thank Doctors F. Brink, N. B. Gilula, A. Mauro, and P. Siekevitz for allowing us to use laboratory equipment and supplies and for their critical reading of this manuscript.

This research was supported by research grants, CRBS 248 from the National Foundation-March of Dimes and VC 153 from the American Cancer Society to Dr. Diacumakos, and funds to Dr. Giulian from an NIH Training grant, GM 01789.

*Received for publication 8 March 1976, and in revised form 2 July 1976.*

## REFERENCES

1. Adrian, R. H. 1956. The effect of internal and external potassium concentration on the membrane potential of frog muscle. *J. Physiol. (Lond.).* **133:** 631–658.
2. Arstila, A. U., H. O. Jauregui, J. Chang, and B. F. Trump. 1971. Studies on cellular autophagocytosis. *Lab. Invest.* **24:**162–174.
3. Aull, F. 1966. Measurement of the electrical potential difference across the membrane of the Ehrlich mouse ascites tumor cell. *J. Cell. Physiol.* **69:**21–32.
4. Bard, J., and E. Wright. 1974. The membrane potentials of fibroblasts in different environments. *J. Cell. Physiol.* **84:**141–146.
5. Borle, A. B., and J. Loveday. 1968. Effects of temperature, potassium, and calcium on the electrical potential difference in HeLa cell. *Cancer Res.* **28:**2401–2405.
6. Cockrell, R. E., E. J. Harris, and B. C. Pressman. 1966. Energetics of potassium transport in mitochondria induced by valinomycin. *Biochemistry.* **5:**2326–2334.
7. Dalton, A. J., and M. D. Felix. 1954. Cytologic and cytochemical characteristics of the Golgi substance of epithelial cells of the epididymus—in situ, in homogenates and after isolation. *Am. J. Anat.* **94:**171–208.
8. Diacumakos, E. G. 1973. Methods for micromanipulation of human somatic cells in culture. *Methods Cell Biol.* **8:**287–311.
9. Erlandson, R. A., and E. de Harven. 1971. The ultrastructure of synchronized HeLa cells. *J. Cell Sci.* **8:**353–397.

10. FARQUHAR, M. G., and G. E. PALADE. 1962. Functional evidence for existence of a third cell type in the renal glomerulus. *J. Cell Biol.* **13**:55–87.
11. GEDDES, L. A. 1971. *In* Electrodes and the Measurement of Bioelectric Events. John Wiley & Sons, Inc., New York. 154–184.
12. HARRIS, E. J., and B. C. PRESSMAN. 1969. The direction of polarity of the mitochondrial transmembrane potential. *Biochim. Biophys. Acta.* **172**:66–70.
13. KATER, S. B., and C. NICHOLSON, editors. 1973. Intracellular Staining in Neurobiology. Springer-Verlag New York Inc., New York.
14. KROEGER, H., and M. LEZZI. 1966. Regulation of gene action in insect development. *Annu. Rev. Entomol.* **11**:1–22.
15. LAVELLEE, M., O. F. SCHANNE, and N. C. HEBERT, editors. 1969. Glass Microelectrodes. J. Wiley & Sons, Inc., New York. 446 pp.
16. LING, G., and R. W. GERARD. 1949. The normal membrane potential of frog sartorius fibers. *J. Cell. Comp. Physiol.* **34**:383–396.
17. LOEWENSTEIN, W. R., and Y. KANNO. 1963. The electrical conductance and potential across the membrane of some cell nuclei. *J. Cell Biol.* **16**:421–425.
18. LOEWENSTEIN, W. R., and Y. KANNO. 1963. Some electrical properties of a nuclear membrane examined with a microelectrode. *J. Gen. Physiol.* **46**:1123–1140.
19. LUDFORD, R. J., J. SMILES, and F. V. WELCH. 1948. The study of living malignant cells by phase contrast and ultra-violet microscopy. *J. R. Microsc. Soc.* **68**:1–9.
20. LUDFORD, R. J., and J. SMILES. 1950. Cytological characteristics of fibroblasts and sarcoma cells demonstrable by phase-contrast microscopy. *J. R. Microsc. Soc.* **70**:186–193.
21. MITCHELL, P. 1967. Proton-translocation phosphorylation in mitochondria, chloroplasts, and bacterial: natural fuel cells and solar cells. *Fed. Proc.* **26**:1370–1379.
22. MONNE, L. 1939. Polarisationsoptische Untersuchungen über den Golgi-Apparat und die Mitochondrien männlicher Geschlechts-Zellen einiger Pulmonaten-Arten. *Protoplasma.* **32**:184–192.
23. MUNN, E. A., editor. 1974. The Structure of Mitochondria. Academic Press, Inc., New York. 43–50.
24. NAORA, H., H. NAORA, M. IZAWA, V. G. ALLFREY, and A. E. MIRSKY. 1962. Some observations on differences in composition between the nucleus and cytoplasm of the frog oocyte. *Proc. Natl. Acad. Sci. U. S. A.* **48**:853–859.
25. REDMANN, K., CH. STOTTE, and D. LUDERS. 1967. Membranpotential-Messungen an KB-Zellculturen. *Naturwissenschaften.* **54**:255.
26. ROBBINS, E., and N. K. GONATAS. 1964. Histochemical and ultrastructural studies on HeLa cell cultures exposed to spindle inhibitors with special reference to the interphase cell. *J. Histochem. Cytochem.* **12**:704–711.
27. SANTINI, M., editor. 1975. Golgi Centennial Symposium. Raven Press, New York. 668 pp.
28. TUPPER, J. T., and H. TEDESCHI. 1969. Microelectrode studies on the membrane properties of isolated mitochondria. *Proc. Natl. Acad. Sci. U. S. A.* **63**:370–377.